

Guiding in the visible with “colorful” solid-core Bragg fibers

Alexandre Dupuis,[†] Ning Guo,[†] Bertrand Gauvreau, Alireza Hassani, Elio Pone, Francis Boismenu, and Maksim Skorobogatiy^{*}

École Polytechnique de Montréal, Génie Physique, C.P. 6079, succursale Centre-Ville Montreal, Québec H3C3A7, Canada

**Corresponding author: maksim.skorobogatiy@polymtl.ca*

Received May 31, 2007; revised August 22, 2007; accepted September 1, 2007; posted September 5, 2007 (Doc. ID 83616); published September 28, 2007

We report on the fabrication and characterization of solid-core all-polymer Bragg fibers consisting of a large-diameter polymethyl methacrylate (PMMA) core surrounded by 50 alternating PMMA/polystyrene (PS) polymer layers. By modifying the reflector layer thickness we illustrate that bandgap position can be adjusted at will in the visible. Moreover, such fibers are intensely colored in both the transmission and the outside reflection modes. Potential applications of such fibers are discussed. © 2007 Optical Society of America

OCIS codes: 060.2280, 060.2270.

Microstructured plastic optical fibers have been recently applied to various important problems, including data communication [1–3], nonlinear optics [4], light amplification [5], sensors [6–8], THz guiding [9,10], and biocompatible fibers for *in vivo* light delivery and sensing [11,12].

In this Letter, we present the fabrication and optical characterization of a solid-core photonic crystal all-polymer Bragg fiber for guiding in the visible range. The fiber is designed in view of its potential applications in plasmonic fiber-based sensors [8], high-bandwidth datacom links [3], and color-selective illumination.

The fibers detailed in this Letter consist of a large polymethyl methacrylate (PMMA) core surrounded by a 50 layer PMMA/polystyrene (PS) Bragg reflector of refractive index contrast $\sim 1.49/1.59$. A co-rolling process [13] was used to make the fiber preform. Large bandgaps (spectral width of up to $\sim 25\%$ of a bandgap center wavelength) were predicted for this material combination. Fibers with distinct realizations of photonic bandgaps were fabricated by drawing the same preform into fibers of various outside diameter.

The fiber preform [Fig. 1(a)] was prepared using commercial plastic rods and films. Particularly, PMMA film, PS film, and PMMA rods were purchased from the Degussa Company, the Dow Chemical Company, and McMaster Carr Canada, respectively. The core consisted of a 1.27 cm diameter PMMA rod that was degassed and annealed in an oven at 90°C for 48 h prior to use. PS and PMMA films, both of 50 μm thickness, were then co-rolled around a PMMA core rod to create 50 alternating PS/PMMA layers (Bragg reflector). The fiber preform was consolidated in an oven at 130°C for 4 h. The preform was then mounted in a draw tower and pre-heated at 150°C for 2 h. Finally, the fiber was drawn at 180°C at a speed of 1 m/min. Figure 1(b) shows a microscope image of the fiber cross section with Bragg reflector layers clearly visible.

The fiber was drawn from the same preform down to several different diameters, ranging from

100 to 350 μm , with the aim of varying the spectral position of the photonic bandgap. Transmission through ~ 20 cm of such fibers was then studied using a supercontinuum white-light source focused by an objective into the fiber center. Observation of the fibers revealed that upon launching white light, all its spectral components not guided by the reflector bandgap were irradiated in the first 1–3 cm along the fiber length. Subsequently, only a particular color guided by the bandgap was propagated to the fiber end (Fig. 2). Moreover, due to imperfections, side-scattering loss in such fibers is substantial, thus leading to coloring of the whole fiber by the guided color.

The fiber photonic bandgaps were then independently observed by recording the fiber transmission spectra with the aid of a monochromator. Figure 3(a) presents the fiber transmission spectra in the visible region normalized by the power spectrum of a supercontinuum source. Fiber segments having outside/core diameters of 350/250, 210/145, 170/103, and

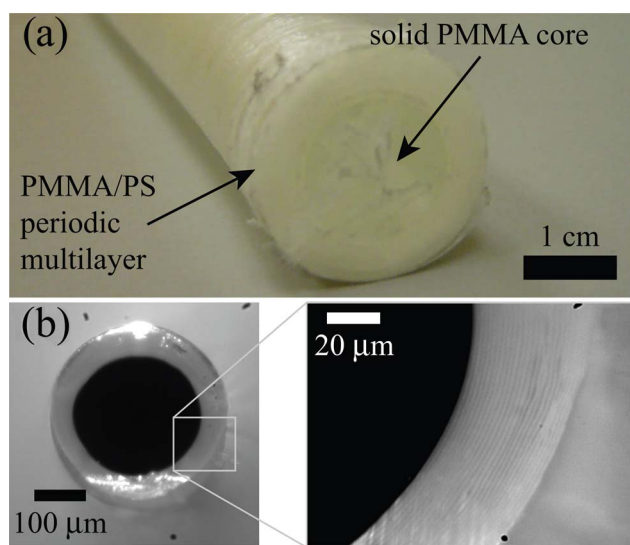
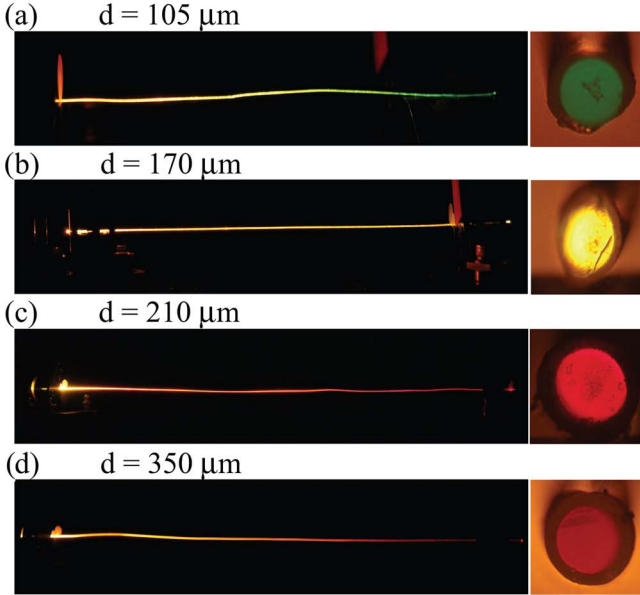


Fig. 1. (Color online) (a) Bragg fiber preform featuring a solid PMMA core and a 50 layer PMMA/PS reflector. (b) Optical micrograph of the drawn fiber cross section.

PMMA/PS Bragg fiber:



Reference PMMA/PMMA fiber:

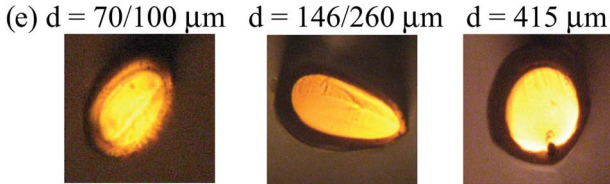


Fig. 2. (Color online) Photographs of the side-scattered and transmitted light for fibers of different diameters when excited by a supercontinuum white-light source. (a)–(d) PMMA/PS Bragg fiber, (e) reference PMMA/PMMA fiber.

$105/77 \mu\text{m}$ guide reddish-orange, red, yellow, and green light, respectively. The corresponding fiber lengths studied were 27.2, 27.2, 9.5, and 5.8 cm, respectively. It is worth noting that the human perception of color is quite complex. Thus, for example, while the spectral transmission peak of the $350 \mu\text{m}$ diameter fiber is at red (660 nm), the actual color perceived by the eye is orange due to the presence of a second peak in the green (540 nm). Overestimation of the solid-core Bragg fiber losses from the corresponding normalized spectra gives 0.6–4 dB/cm fiber loss depending on the sample. As we will show later, the main contribution to such loss in the near IR is a PMMA absorption loss, while in the visible it is scattering off the fiber imperfections, which, in principle, can be greatly reduced through perfecting the preform fabrication process. Simulations of the fiber transmission properties revealed that all the fibers are guided by the higher-order photonic bandgaps.

Interpretation of the spectra in Fig. 3(a) is not trivial, as several loss mechanisms are contributing simultaneously. To demonstrate the interplay of the major physical phenomena responsible for a particular shape of a transmission spectrum, in Fig. 3(b) we consider, in detail, the case of a Bragg fiber with a diameter of $350 \mu\text{m}$.

We start with the near-IR region above 1000 nm, where all the spectral peaks can be explained by the

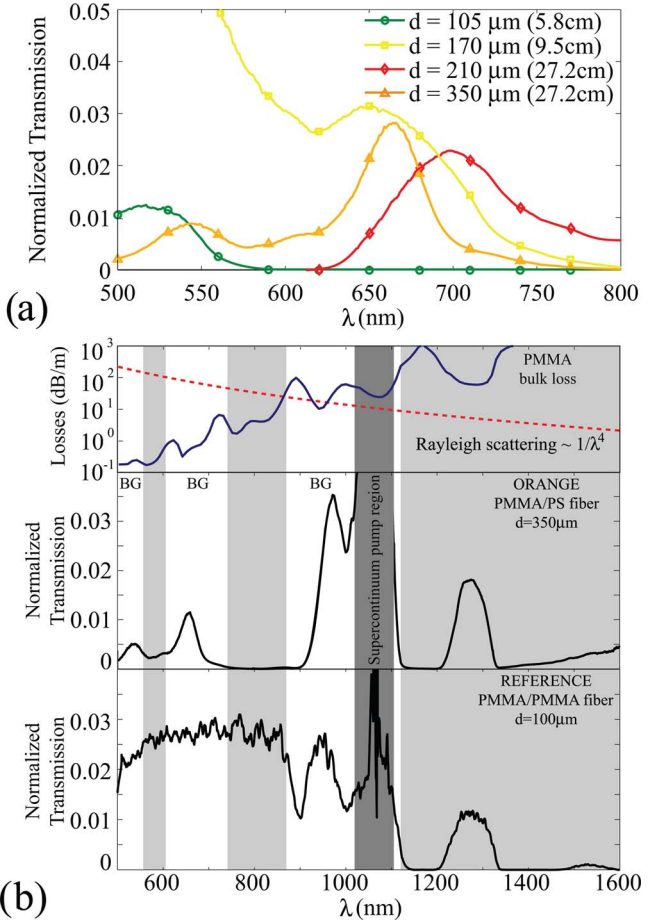


Fig. 3. (Color online) Transmission spectra of fibers of different diameters, normalized with respect to a supercontinuum source. (a) Visible spectra, (b) visible and near-IR spectra for a $350 \mu\text{m}$ diameter PMMA/PS Bragg fiber and a $100 \mu\text{m}$ diameter PMMA/PMMA reference fiber.

shape of a PMMA material loss curve alone. In the top part of Fig. 3(b), bulk loss of a PMMA material is presented as a solid curve. Note that, in the near-IR region above 900 nm, PMMA loss increases considerably, with the exception of several transparency windows located around 950, 1050, and 1300 nm. The presence of such material transparency windows results in enhanced fiber transmission in their vicinity. Regardless of the existence of a reflector bandgap, the absolute amplitudes of the 1050 and 1300 nm peaks can be fitted extremely well by using only the values of a PMMA material loss and a fiber span length. The success of such a fit is easy to understand, as in the absence of scattering loss, whether guided by the bandgap or not, the mode field will be localized mostly in the PMMA material of a core; therefore modal loss will be defined solely by the PMMA material loss.

To account for the high loss in the visible region we assume a strong contribution due to Rayleigh scattering off imperfections. Particularly, for the preform fabrication method by co-rolling of two plastic films, slippage, distortion, reflector layer “wrinkling” during the consolidation process, as well as dust and air bubble accumulation on the interfaces between the films are difficult to mitigate, thus ultimately de-

riorating the quality of a resultant fiber. To account for the scattering loss from such imperfections, in the top part of Fig. 3(b) a Rayleigh scattering curve (dotted) $70 \text{ [dB/m]} \times (660 \text{ nm}/\lambda \text{ [nm]})^4$ is presented. The parameters of this curve were chosen to fit the amplitude of a spectral peak at 660 nm.

To demonstrate that PMMA absorption and Rayleigh scattering are insufficient to explain all the structural features of the Bragg fiber transmission spectra in the visible, we fabricated a reference fiber made entirely of PMMA. To more faithfully reproduce the type of fiber nonuniformities that arise during the fabrication method of the Bragg fiber, we opted to roll a PMMA film around a PMMA rod and to draw the resulting structure. The PMMA film and the PMMA rod were the same as those used for the PMMA/PS Bragg fiber fabrication. The PMMA reference fiber was then drawn to different diameters ranging from 100 to 415 μm ; see Fig. 2(e). All these fibers scattered and transmitted light that appeared orange to the naked eye and had similar, diameter independent, transmission spectra. We attributed apparent guidance in the PMMA core to the high scattering loss in the all-PMMA reflector region. The transmission spectrum of a PMMA reference fiber of 70/100 μm diameter and 12.9 cm length is presented in Fig. 3(b) and can be explained by considering the above-mentioned PMMA absorption and Rayleigh scattering. With only these two loss mechanisms present, one expects a relatively featureless spectrum in the visible and a transmission maximum around 800–900 nm.

We, therefore, concluded that the unusual spectral features of the Bragg fibers in the visible can only be explained by the presence of the reflector bandgaps. Particularly, when guiding inside of a bandgap, most of the light is concentrated in the fiber core, with only a small fraction present in the reflector. Scattering at the interface between the fiber core and a first reflector layer is then described by the previously mentioned Rayleigh formula. For the wavelengths outside of a bandgap, the modal field penetrates deeply into the imperfect reflector layers; therefore scattering loss increases dramatically, and the core mode is effectively lost.

We now investigate the exact position of the bandgaps. From analysis of the micrographs of the $d = 350 \mu\text{m}$ fiber cross sections we determine that the average PMMA/PS bilayer thickness is 2084 nm. Moreover, in the preform the ratio of the PMMA/PS layer thicknesses is 1:1, while in the fibers the ratio seems to change toward increased relative PS thickness. Relative thickening of the PS layers compared with those of PMMA can be, in principle, justified by the considerably lower viscosity of PS. Bandgap regions centered around the transmission peaks in the visible [transparent windows in Fig. 3(b)] marked as

BG] were achieved theoretically by assuming 625 nm/1459 nm layer thicknesses of a PMMA/PS multilayer. Although this thickness ratio is larger than that recorded from the micrographs, it nevertheless prescribes correctly the bandgap positions. The discrepancy between the theoretical and experimental thickness ratios is still under investigation, with potential explanations being nonuniformity and chirping of the layer thickness during the perform fabrication and draw process, as well as uncertainty in the knowledge of the polymer refractive indexes.

In conclusion, we demonstrated bandgap guidance in solid-core Bragg fibers operating in a visible range. Bandgap position was adjusted by drawing fibers of different outside diameters, and various colors coming out of the fibers were recorded when excited with a white-light source. Fiber losses in the near IR are dominated by the PMMA material loss, while in the visible they are dominated by scattering off reflector imperfections.

This work was supported by the Canada Research Chair and Canada Institute for Photonics Innovations.

[†]These authors have contributed equally to the paper.

References

- Y. Koike, T. Ishigure, and E. Nihei, *J. Lightwave Technol.* **13**, 1475 (1995).
- M. A. van Eijkelenborg, A. Argyros, A. Bachmann, G. Barton, M. C. J. Large, G. Henry, N. A. Issa, K. F. Klein, H. Poisel, W. Pok, L. Poladian, S. Manos, and J. Zagari, *Electron. Lett.* **40**, 592 (2004).
- M. Skorobogatiy and N. Guo, *Opt. Lett.* **32**, 900 (2007).
- D. W. Garvey, K. Zimmerman, P. Young, J. Tostenuude, J. S. Townsend, Z. Zhou, M. Lobel, M. Dayton, R. Wittorf, M. G. Kuzyk, J. Sounick, and C. W. Dirk, *J. Opt. Soc. Am. B* **13**, 2017 (1996).
- K. Kuriki, Y. Koike, and Y. Okamoto, *Chem. Rev.* **102**, 2347 (2002).
- C. M. B. Cordeiro, M. A. R. Franco, G. Chesiini, E. C. S. Barreto, R. Lwin, C. H. Brito Cruz, and M. C. J. Large, *Opt. Express* **14**, 13056 (2006).
- A. Argyros, M. A. van Eijkelenborg, M. C. J. Large, and I. M. Bassett, *Opt. Lett.* **31**, 172 (2006).
- A. Hassani and M. Skorobogatiy, *J. Opt. Soc. Am. B* **24**, 1423 (2007).
- H. Han, H. Park, M. Cho, and J. Kim, *Appl. Phys. Lett.* **80**, 2634 (2002).
- M. Skorobogatiy and A. Dupuis, *Appl. Phys. Lett.* **90**, 113514 (2007).
- A. Dupuis, N. Guo, Y. Gao, N. Godbout, S. Lacroix, C. Dubois, and M. Skorobogatiy, *Opt. Lett.* **32**, 109 (2007).
- G. Emiliyanov, J. B. Jensen, O. Bang, A. Bjarklev, P. E. Hoiby, L. H. Pedersen, E. Kjaer, and L. Lindvold, *Opt. Lett.* **32**, 460 (2007).
- Y. Gao, N. Guo, B. Gauvreau, M. Rajabian, O. Skorobogata, E. Pone, O. Zabeida, L. Martinu, C. Dubois, and M. Skorobogatiy, *J. Mater. Res.* **21**, 2246 (2006).